Rate-Dependent Slip of Newtonian Liquid at Smooth Surfaces

Yingxi Zhu and Steve Granick

Department of Materials Science and Engineering, University of Illinois, Urbana, Illinois 61801

(Received 6 February 2001; published 10 August 2001)

Newtonian fluids were placed between molecularly smooth surfaces whose spacing was vibrated at spacings where the fluid responded as a continuum. Hydrodynamic forces agreed with predictions from the no-slip boundary condition only provided that flow rate (peak velocity normalized by spacing) was low, but implied partial slip when it exceeded a critical level, different in different systems, correlated with contact angle (surface wettability). With increasing flow rate and partially wetted surfaces, hydrodynamic forces became up to 2–4 orders of magnitude less than expected by assuming the no-slip boundary condition that is commonly stated in textbooks.

DOI: 10.1103/PhysRevLett.87.096105 PACS numbers: 68.08.–p, 68.35.Md

A tenet of textbook continuum fluid dynamics is the "no-slip" boundary condition, which means that fluid molecules immediately at the surface of a solid move with exactly the same velocity as that solid. Feynman noted in his lectures that the no-slip condition explains why large particles are easy to remove by blowing past a surface, but small particles are not. After much controversy during the 19th century [1], the possibility of slip was discussed until recently, in mainstream literature, only in the context of the flow of polymer melts [2,3], though over the years persistent doubts were expressed [4]. No slip contrasts with "slip" characteristic of highly viscous polymers [2,3], monolayers of gas condensed on vibrated solids [5], superfluid helium [6], moving contact lines of liquid droplets on solids [7], and kinetic friction of liquid films less than 5–10 molecular dimensions thick [8]. In addition, recent simulations [9,10] and experiments [11,12] concluded that low-viscosity fluids slip past smooth surfaces if they are partially wetted. This is consistent with a large but controversial body of earlier experimental literature, mainly based on flow through hydrophobic pores [4]. In all of this work, the common assumption was that the amount of slip (the "slip length"; see below) was a constant. Apart from computer simulations [13,14], velocity dependence of slip was not expected, but those simulations were performed at shear rates higher than could be achieved in a laboratory.

Here we present what we believe to be the first direct measurements in which velocity of the moving liquid is varied over a wide range and conclude that (i) the amount of slip depended strongly on velocity; (ii) the onset of slip varied systematically with contact angle.

Two solids of mean radius of curvature R ($\approx$2 cm in the experiments reported below), at spacing D, experience a hydrodynamic force F_H as they approach (or retreat from) one another, thereby squeezing fluid out of (or into) the intervening gap. This force is proportional to the rate at which spacing changes, dD/dt (t denotes time), is proportional to the viscosity, η (assumed to be constant), and is inversely proportional to D. The no-slip boundary condition combined with the Navier-Stokes equations gives to first order the following expression, known as the Reynolds equation:

$$F_H = f^* 6\pi R^2 \eta (1/D)(dD/dt), \tag{1}$$

and high-order solutions essentially confirm this, the lowest-order term [15]. We introduce f^*, the dimensionless number that quantifies, if $f^* \neq 1$, deviation from the classical prediction. The prediction is analogous when the surface spacing is vibrated [12]. Then a sinusoidal oscillatory drive generates an oscillatory force whose peak we will denote as $F_{H,\mathrm{peak}}$. The peak velocity is $\nu_{\mathrm{peak}} = d\omega$ where d is vibration amplitude and ω is the radian frequency of vibration.

Nanometer-level oscillatory modulations of film spacing were performed when a drop of liquid was placed between molecularly smooth surfaces of mica within a modified surface forces apparatus. The amplitude and frequency were controlled independently, allowing the mean velocity to vary over a wide range without large change of the film thickness. Details of the apparatus were described elsewhere [16]. We analyze here the viscous response, 90° out of phase with the sinusoidal drive. The signal at 0° phase shift can be used to determine the conservative forces, as we have done elsewhere [16].

The meniscus forces that contribute to dynamic force measurements on rough surfaces did not appear to contribute. On rough surfaces, they augment the dissipation above that expected from hydrodynamic flow between smooth surfaces [17]—but in this study, using smooth surfaces, we found that forces were *reduced below* that level (see below). The spring constant of the force-measuring assembly also influences the phase if the spring constant is less than the force constant measured [17,18], but this was not so for the present experiments.

Three liquid-solid systems were studied. In order of increasing contact angle, these were (i) tetradecane against adsorbed surfactant; (ii) tetradecane against a methyl-terminated self-assembled monolayer (SAM); (iii) water

against the same methyl-terminated SAM. For cases (ii) and (iii), atomically smooth, step-free muscovite mica was coated, using methods described elsewhere [18], with a methyl-terminated close-packed monolayer of condensed octadecyltriethoxysiloxane (OTE). The methods were improved by vacuum distilling the OTE (Aldrich) before use. For case (i), 0.2 wt % of 1-hexadecylamine surfactant, $CH_3(CH_2)_{15}NH_2$ (Aldrich, 99% pure), was added to tetradecane, dried over molecular sieves, and allowed to adsorb onto mica. On OTE, the advancing contact angle of water was $\approx 110^\circ$ and that of tetradecane $\approx 44^\circ$. Hysteresis was $<1-2^\circ$. For case (i), the advancing contact angle was $\approx 12^\circ$.

First we consider tetradecane, an oil whose low viscosity is close to that of water. Figure 1 (top panel) compares the flow of tetradecane between mica on the one hand (wetting) and OTE (partially wetting). In the former case, the data obey Eq. (1) with the classical continuum prediction quantitatively ($f^* = 1$). This confirms prior surface forces-based experiments by other groups [19] and lends credibility to the new results that follow.

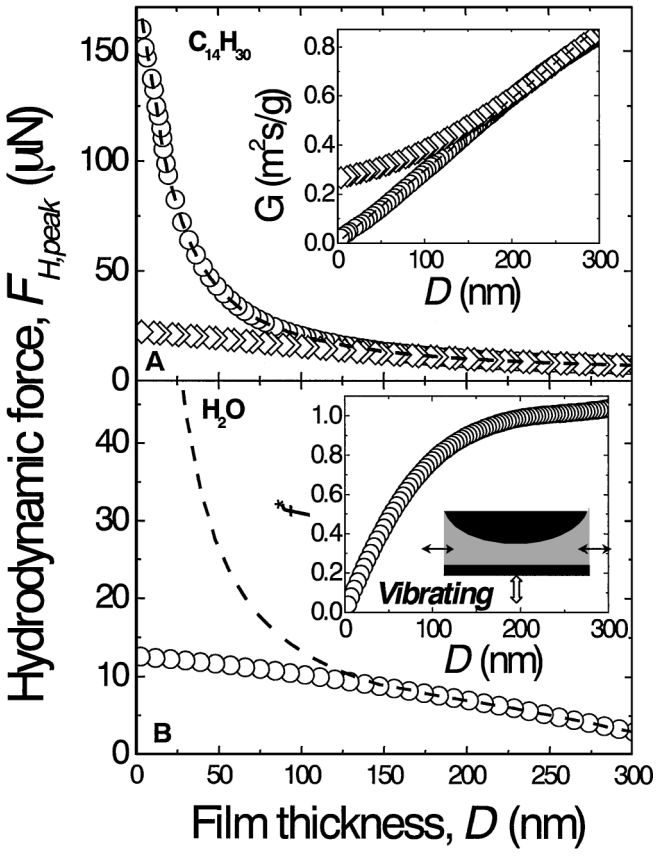

FIG. 1. Hydrodynamic force between crossed cylinders. $F_{H,\text{peak}}$, is plotted against surface separation D for tetradecane (upper panel) and deionized water (bottom panel) undergoing 1 nm spacing vibrations at 63 rad s^{-1}. In the top panel, the surface was wetting (mica; circles) or partially wetting with contact angle $\approx 44^\circ$ (OTE; diamonds). A schematic diagram of the experiments is shown in the bottom panel. The data are compared to the hydrodynamic force expected from the no-slip boundary condition, Eq. (1) (dashed lines). The inset of each panel shows the damping function, $G = (6\pi R^2 \nu_{\text{peak}})/F_{H,\text{peak}} = D/\eta$, plotted against D. The reciprocal of the slope in the linear portion of the inset gives the known viscosity of these fluids. Given the no-slip boundary condition and a Newtonian fluid, G should extrapolate to the origin.

New results were found when tetradecane was placed between partially wetting surfaces (OTE). Spacing, D, was measured as the thickness between the organic monolayers, each 2.4 nm thick. It is obvious that, at spacings <0.1 μm, the hydrodynamic forces were systematically less than for the wetting situation. To show this more clearly, the inset shows a linearization of Eq. (1). A quantity proportional to $1/F_{H,\text{peak}}$ is plotted against D: whereas the data obtained at the largest spacings extrapolate linearly to the origin, which is expected from the no-slip boundary condition; they deviate decidedly at lesser spacings, indicating lesser resistance to flow. The tetradecane molecule is tiny compared to the surface spacing, so confinement-induced anomalies [8] are not expected. It is as if the hydrodynamic force reached a saturation level beyond which only a limited amount of further increase was possible. Equilibrium surface forces appear in an alkane system only at much lesser separation, $D < 3-5$ nm [20]. They were zero at the spacings that were studied and so presented no complication.

The generality of this behavior is suggested by the fact that deionized water (Nanopure II) gave results that were qualitatively similar, as shown in Fig. 1 (bottom panel). It is true that there exist long-range forces in the equilibrium force-distance profiles of water between hydrophobic surfaces [21] (but their range is dramatically reduced when the hydrophobic surfaces are in relative motion [22]) so the observation in water may at first seem to be less definitive. That this is not fundamental becomes clear when one considers that a static force profile is equilibrated and therefore corresponds to a response *in-phase* with sinusoidal vibrations of the surface spacing—unlike the dissipative forces analyzed here.

To take stock, these observations cannot be explained away by appeal to modification of the fluid viscosity itself owing to shear thinning, since the case of tetradecane between mica at comparable levels of thickness (complete wetting) presents a counterexample to that. The experiments were performed at least 6 orders of magnitude below the very high shear rates at which shear thinning of small alkane molecules is anticipated based on computer simulations, so shear thinning is hardly credible. These observations cannot be explained away by appealing to compliance of the OTE or surfactant monolayers; these have been measured to be very stiff [8].

It is not clear that Eq. (1), which was derived for the no-slip boundary condition, should be expected to be obeyed in the case of partial slip. It is useful, however, to express deviations from it as a fitting parameter to which we do not assign physical meaning. The parameter, f^*,

defined in Eq. (1), was calculated. Figure 2 illustrates its rate dependence for the water system (effects were similar for tetradecane, as summarized by the master curves presented in Fig. 3). It is plotted against separation for four different values of peak velocity. One sees that the extent of deviation from the classical prediction increased with increasing velocity, even with film thickness held constant. The deviations are so large that it is necessary to plot them on a logarithmic scale.

There is a tradition in fluid dynamics to infer the slip length, the fictive distance inside the solid at which the no-slip flow boundary condition would hold. Without necesarily assigning physical meaning to this quantity, it can be used as an alternative expression of the same data. Mathematical manipulation [23] shows that f^* and slip length (b) are related as

$$f^* = 2 \times \frac{D}{6b}\left[\left(1 + \frac{D}{6b}\right)\ln\left(1 + \frac{6b}{D}\right) - 1\right]. \quad (2)$$

Results (Fig. 3) show that the slip length was variable. This contrasts with the common theoretical assumption that the slip length of low-viscosity fluids is a constant number.

In Fig. 3, one sees that the data appear to collapse when f^* was compared at the same flow rate, i.e., the same ratio of velocity to film thickness. The (equivalent) changes of slip length are also shown. In this comparison, the peak velocity was varied by more than 2 orders of magnitude, as described in the caption of Fig. 3, and the film spacing was varied by a factor of nearly 6. The largest deviations were observed for deionized water between OTE-coated surfaces. Lesser deviations were seen for tetradecane between OTE-coated surfaces and the smallest for surfaces modified with adsorbed surfactant. In this latter case, the chemical makeup of the solid surfaces was modified by physisorption rather than by chemical reaction.

It is worth emphasizing the latter system. The simple strategy, dissolving surface-active molecules at dilute concentration within fluid at an otherwise-wetting surface, also caused predictions based on no-slip boundary conditions to break down in a velocity-dependent way. This suggests a possible explanation for the success of "friction modifiers" [20], in oil and gasoline — a process about whose mechanism engineers have long speculated.

There are at least two alternative scenarios of microscopic interpretation. First, the fluid viscosity might depend on distance from the wall. Fits to continuum-based predictions kindly supplied by Brady [24] show that the data at

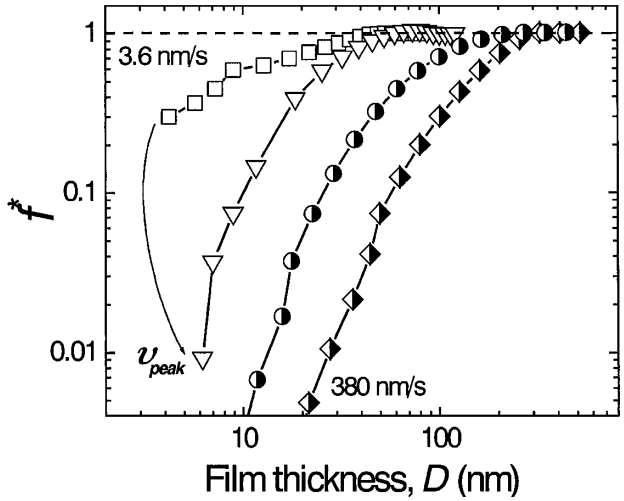

FIG. 2. On log-log scales, f^* is plotted against D for deionized water between partially wetting (OTE-coated) at peak velocity 3.6 nm s^{-1} (squares, 1 Hz), 40 nm s^{-1} (triangles, 1 Hz), 100 nm s^{-1} (circles, 10 Hz), and 380 nm s^{-1} (diamonds, 10 Hz). Given the no-slip boundary condition, $f^* = 1$. To observe $f^* < 1$ shows that flow was easier than expected from that assumption.

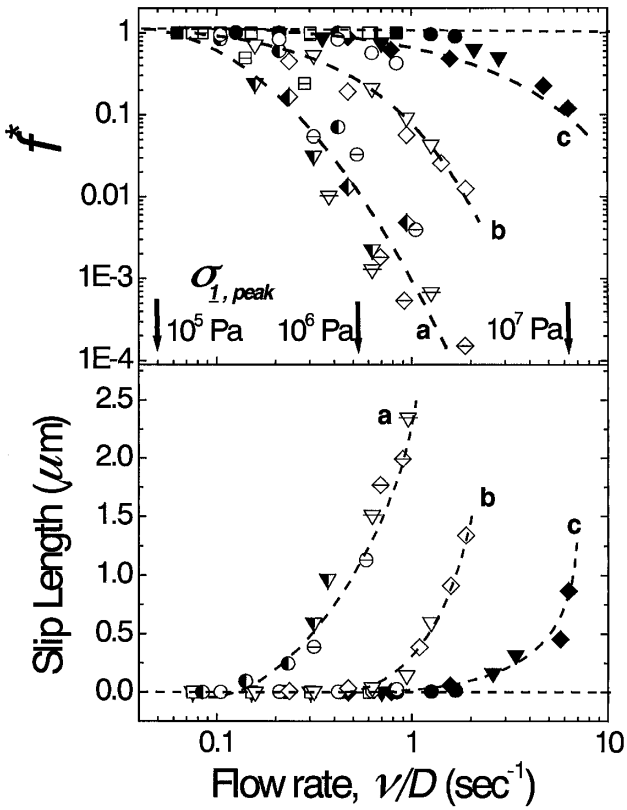

FIG. 3. On log-log scales, f^* (top panel) is plotted against ν_{peak}/D for (a) deionized water between OTE (cross or semifilled symbols), contact angle ≈110°, (b) tetradecane between OTE (open symbols), contact angle ≈44°, and (c) tetradecane containing 0.2% hexadecylamine between mica (filled symbols), contact angle ≈12°. At the thickness 50 nm (squares), 24 nm (circles), 18 nm (triangles), and 8 nm (diamonds), the frequency was 6.3 rad s^{-1} or 63 rad s^{-1} (cross-filled symbols). The peak hydrodynamic stresses of 10^5, 10^6, and 10^7 Pa are indicated at the corresponding flow rate points on the abscissa. The bottom panel compares the slip length, which is equivalent to f^* as described in text. Shear rate is, if the stick boundary condition holds, proportional to flow rate in a crossed cylinder geometry by a geometrical factor of magnitude between 10^3 and 10^4 that depends on D [26], $\gamma_{max} = A\sqrt{R/D}\,v_{peak}/D$, where $A = (27/128)^{1/2}$.

high flow rates are consistent with a two-layer-fluid model in which a layer 0.5 nm thick, but with viscosity 10–20 times *less* than the bulk fluid, adjoins each solid surface (the film thickness and its viscosity are fitting parameters in such a calculation). A possible mechanism to explain its genesis was proposed by de Gennes (see below).

Alternatively, from the empirically derived slip length, known models permit one to calculate the implied peak hydrodynamic stress on the coincident center of the two cylinders [23] (this is believed to determine slip in polymer melts [3] and monolayers sliding on solids [5]). With this in mind, the abscissa of Fig. 3 contains arrows showing the implied peak pressure at three increasing levels of flow rate, each differing by an order of magnitude. The moving surfaces appeared to decouple at lower-and-lower integrated stresses, the larger the contact angle. This is reasonable since the contact angle quantifies the degree to which molecules of fluid attract one another more strongly than the surface.

de Gennes (private communication) proposes that the reason for velocity dependence may be that shear induces the nucleation of vapor bubbles; once the nucleation barrier is exceeded, the bubbles grow to cover the surface, and flow of liquid is over this thin gas film rather the solid surface itself. The model predicts that the critical flow rate (shear rate) for onset of bubble nucleation is proportional to the cube of the bubble's contact angle, which is qualitatively consistent with the data. Shear rate is larger than flow rate by a large geometrical factor (see caption of Fig. 3).

In summary, failure of predictions based on the classical no-slip boundary condition of fluid flow has been demonstrated in three liquid-solid systems. In order of increasing contact angle, these were (i) tetradecane against adsorbed surfactant; (ii) tetradecane against a methyl-terminated self-assembled monolayer; and (iii) water against the same methyl-terminated SAM. It is not yet known to what extent the presence of surface roughness (chemical or topographical) might modify these effects [11,25] (experiments in this direction are in progress).

The present experiments with molecularly smooth surfaces appear to present a touchstone against which to compare theories of momentum transfer in fluid flow. They have implications in areas such as filtration, colloidal dynamics, and microfluidic devices, and might form the basis of a strategy for saving energy in the transport of fluids such as oil and gasoline.

We are indebted for invaluable discussions to J. F. Douglas and P.-G. de Gennes, and to J. F. Brady, O. I. Vinogradova, and J. L. Barrat for commenting on the manuscript. This work was supported by the National Science Foundation (Tribology Program) and by facilities of the U.S. Department of Energy, Division of Materials Science, under Award No. DEFG02-91ER45439 through the Frederick Seitz Materials Research Laboratory at the University of Illinois at Urbana-Champaign.

[1] S. Goldstein, *Modern Developments in Fluid Dynamics* (Clarendon, Oxford, 1938), Vol. II, pp. 677–680.
[2] P.-G. de Gennes, C.R. Acad. Sci. B **288**, 219 (1979).
[3] L. Léger, E. Raphael, and H. Hervet, Adv. Polym. Sci. **138**, 185 (1999).
[4] For a review, see O. I. Vinogradova, Int. J. Miner. Process. **56**, 31 (1999).
[5] C. Mak and J. Krim, Phys. Rev. B **58**, 5157 (1998).
[6] S. M. Tholen and J. M. Parpia, Phys. Rev. Lett. **67**, 334 (1991).
[7] C. Huh and L. E. Scriven, J. Colloid Interface Sci. **35**, 85 (1971).
[8] G. Reiter, A. L. Demirel, and S. Granick, Science **263**, 1741 (1994); G. Reiter, A. L. Demirel, J. S. Peanasky, L. Cai, and S. Granick, J. Chem. Phys. **101**, 2606 (1994).
[9] P. A. Thompson and M. O. Robbins, Phys. Rev. A **41**, 6830 (1990).
[10] J.-L. Barrat and L. Bocquet, Phys. Rev. Lett. **82**, 4671 (1999).
[11] R. Pit, H. Hervet, and L. Léger, Phys. Rev. Lett. **85**, 980 (2000).
[12] S. E. Campbell, G. Luengo, V. I. Srdanov, F. Wudl, and J. N. Israelachvili, Nature (London) **382**, 520 (1996).
[13] P. A. Thompson and S. Troian, Nature (London) **389**, 360 (1997).
[14] M. Cieplak, J. Koplik, and J. R. Banavar, Phys. Rev. Lett. **86**, 803 (2001).
[15] S. Kim and S. Karrila, *Microhydrodynamics* (Butterworth-Heinemann, Newton, MA, 1991).
[16] A. Dhinojwala and S. Granick, Macromolecules **30**, 1079 (1997).
[17] M. C. Friedenberg and C. M. Mate, Langmuir **12**, 6138 (1996); J. Crassous, E. Charlaix, and J.-L. Loubet, Phys. Rev. Lett. **78**, 2425 (1997).
[18] J. S. Peanasky, H. M. Schneider, S. Granick, and C. R. Kessel, Langmuir **11**, 953 (1995).
[19] D. Y. C. Chan and R. G. Horn, J. Chem. Phys. **83**, 5311 (1985); J. N. Israelachvili, J. Colloid Interface Sci. **110**, 263 (1986); J. M. Georges, S. Millot, J. L. Loubet, and A. Tonck, J. Chem. Phys. **98**, 7345 (1993).
[20] K. Walley, K. S. Schweizer, J. Peanasky, and S. Granick, J. Chem. Phys. **100**, 3361 (1994); M. Ruths, H. Ohtani, M. L. Greenfield, and S. Granick, Tribol. Lett. **6**, 207 (1999).
[21] V. S. J. Craig, B. W. Ninham, and R. M. Pashley, Langmuir **14**, 3326 (1998), and references therein.
[22] X. Zhang, Y. Zhu, and S. Granick, J. Am. Chem. Soc. **123**, 6736 (2001).
[23] O. I. Vinogradova, Langmuir **11**, 2213 (1995).
[24] J. F. Brady (private communication).
[25] S. Richardson, J. Fluid Mech. **59**, 707 (1973).
[26] R. G. Horn, O. I. Vinogradova, M. E. Mackay, and N. Phan-Thien, J. Chem. Phys. **112**, 6424 (2000).